JOURNAL OF CATALYSIS **163,** 1–11 (1996)
ARTICLE NO. 0299

Heterogeneous Photocatalytic Oxidation of Trichloroethylene and Toluene Mixtures in Air: Kinetic Promotion and Inhibition, Time-Dependent Catalyst Activity

Yang Luo[1] and David F. Ollis[2]

Department of Chemical Engineering, North Carolina State University, Raleigh, North Carolina 27695-7905

Received March 28, 1995; revised March 27, 1996; accepted March 29, 1996

Photocatalyzed degradation of trace level trichloroethylene (TCE) and toluene in air were carried out over near-UV-illuminated titanium dioxide (anatase) powder in a flow reactor using a residence time of about 5–6 ms. Concentration ranges for TCE and toluene were 0–800 mg/m^3. TCE photooxidation was very rapid under our experimental conditions, and ~100% conversion was achieved for TCE concentration examined up to 753 mg/m^3 as a single air contaminant. Initial photodegradation rates for toluene in humidified air were fitted by a Langmuir–Hinshelwood rate form. Toluene photooxidation sole contaminant rates were of the same order of magnitude as reported previously for *m*-xylene and acetone. No significant intermediates were detected by GC/FID during TCE or toluene photooxidation reactions. Humidification had significant influence: Toluene photooxidation rate increases with the water concentration up to about 1650 mg/m^3 20% relative humidity) and decreases thereafter. The presence of sufficient TCE (225–753 mg/m^3) promoted the toluene photooxidation reaction rate to achieve 90–100% toluene conversion in 5.6 ms. When feed toluene levels measured below ~90 mg/m^3. Higher toluene feed levels "quenched" this TCE promotion effect and also depressed TCE conversion very strongly, but the toluene conversion fell just to the toluene-only levels observed in single contaminant experiments. Photooxidation kinetics of TCE and toluene mixtures in air are thus shown to exhibit strong promotion and inhibition behavior vs that expected from the single-species kinetic degradation data. A previously suggested chlorine radical oxidation of TCE is modified to rationalize the TCE enhancement of the toluene photooxidation rate and the corresponding toluene "quench" of TCE destruction. Time-dependent catalyst activation (by TCE) and deactivation (by toluene or toluene oxidation products and, eventually, even by TCE products) were observed. Carboxylate formation and carboxylic acid accumulation postulated by previous investigators could be a major cause of such catalyst deactivation.

1. INTRODUCTION

Gas–solid photocatalysis has a favorable technical potential to treat a range of air contaminants including aldehydes, alcohols, light hydrocarbons, aromatics, and chlorinated solvents. Photocatalytic oxidation of air contaminants over titanium dioxide has been studied by various research groups over the last two decades. Early photocatalysis explorations included oxidations of alkanes (1–3), isopropanol (1–5), methane (6), secondary alcohols (7), ammonia photooxidation (8), and the decarboxylation of acetic and formic acids (9). Studies providing kinetic rate expressions are those of isobutane partial oxidation (10), 1-butanol photooxidation (11a), and conversions of acetone, 1-butanol, formaldehyde, and *m*-xylene photo oxidation (11b). All of these oxygenate and hydrocarbon studies showed slow to moderate rates of conversion, corresponding to small apparent quantum yields, e.g., of 1–2% for acetone (11b).

In sharp contrast, trichloroethylene photocatalyzed conversion has been found to be near or at 100% even in short residence time (<100 ms) reactors (see summary below). The present research was undertaken to explore if and to what degree the (possible chain) rapid reaction oxidation mechanism of TCE could enhance the photocatalytic oxidation of an aromatic, toluene, which is an important air contaminant from both an ozone formation and noncancer-risk point of view (12).

Trichloroethylene Studies

Trichloroethylene has been examined recently in gas-phase photooxidations by several research groups due to its unusually high photocatalytic quantum yield. Dibble and Raupp systematically explored trichloroethylene photooxidation (13–15) to determine the kinetics of conversion of trace (0–100 ppm) trichloroethylene in air over illuminated TiO_2 using both a fixed-bed reactor and a fluidized bed reactor. The observed reaction rate was a positive to zero apparent order in trichloroethylene and oxygen vapor-phase mole fractions and zero to negative order in water vapor mole fraction, depending on the concentration of each species. Trace water presence was found necessary to maintain photocatalytic catalyst activity for extended periods of time, but higher water levels were strongly inhibitory.

[1] Current address: International Paper, Erie Research Center, 1540 E. Lake Rd. Erie, PA 16533.

[2] To whom correspondence should be addressed.

0021-9517/96 $18.00

Nimlos *et al.* combined mass spectrometry (MS) and Fourier transform infrared (FTIR) spectroscopy to detect directly the important by-products and intermediates of trichloroethylene photocatalyzed conversions over TiO_2 (16). They observed substantial gas-phase chlorinated species including phosgene, molecular chlorine, hydrogen chloride, and dichloroacetyl chloride. Their finding of appreciable levels of both phosgene and molecular chlorine, known in World War I as chemical warfare agents, has stirred concern over photocatalysis by-products in air containing chlorinated olefins.

Holden *et al.* studied photochemical destruction of trichloroethylene in air (17). Trichloroethylene and its photooxidation reaction products were quantified by gas chromatography, coupled gas chromatography–mass spectroscopy, proton nuclear magnetic resonance spectroscopy, infrared spectroscopy, and wet chemical analysis procedures. Their results showed that the destruction of trichloroethylene was complete at slow flow rates (100 ml/min); the major product isolated was dichloroacetyl chloride. At slower flow rates (25 or 10 ml/min), dichloroacetyl chloride was also destroyed to yield a mixture of carbon monoxide, carbon dioxide, chlorine, and phosgene. Small amounts of trichloroethylene epoxide were also detected. These flow rates correspond to approximate reactor residence times of 2.77, 11.1, and 27.7 min, respectively.

Anderson's group examined the dependencies of trichloroethylene photocatalyzed degradation rate on light intensity, feed composition (TCE, O_2, H_2O), and temperature in a bed reactor packed with TiO_2 pellets (18). A monochloroacetate intermediate was identified on the TiO_2 pellet surface via FTIR. The reaction rate is first order with respect to the light intensity, when the reactor is operated with feed mole fractions of 3.7×10^{-5} TCE, 0.02, O_2, 2.3×10^{-3} H_2O, and at a space time of 4.3×10^{-6} g s/mol; space time is defined as the amount of catalyst divided by the inlet TCE molar flowrate. The apparent quantum yield, calculated as the mineralization rate of TCE divided by the incident photon rate, was 4–17% depending upon space time. The trichloroethylene reaction rate was independent of trichloroethylene concentration in the ranges of 37–450 ppm, oxygen mole fraction 0.01–0.2, and water vapor mole fraction 0.001–0.028. The ratio (moles of CO_2 produced)/(moles of TCE degraded) increased to 2, corresponding to the complete mineralization of trichloroethylene to final products CO_2 and HCl, when a temperature of 64°C was used with space time greater than 2.7×10^{-7} g s/mol. Temperature had no effect on trichloroethylene reaction rate in the range of 23 to 62°C. These findings suggest that the complete mineralization of TCE can be obtained simply by increasing the temperature of the photoreactor and the space time. They show that the trichloroethylene reaction rate is independent of flowrate when the conversion is less than 10%, which suggests that the external mass transfer is not controlling the reaction rate.

In a recent kinetic study of trichloroethylene photooxidation, Jacoby constructed a TiO_2 coated annular photoreactor and quantitatively explored the byproducts and intermediates of the trichloroethylene photooxidation (19). He observed that the trichloroethylene reaction can proceed either through the $CHCl_2CClO$ dichloroacetyl chloride (DCAC) intermediate to the final products, CO, CO_2, HCl, $COCl_2$, and trace Cl_2, or through direct photooxidation to form $COCl_2$, HCl, and CO_2. Up to 85% of the reacted trichloroethylene appears as DCAC in the product mixture, indicating the primary importance of the pathway through this intermediate. Both trichloroethylene and DCAC reaction rates can be described by a Langmuir–Hinshelwood rate function. Apparent quantum yields up to 4 (400%) were observed, suggesting a chain reaction mechanism. Jacoby concluded that trichloroethylene destruction was predominantly via a chain reaction that occurs exclusively on the TiO_2 surface. (We review and use this proposed chain mechanism in our discussion of (toluene + TCE) results.) For this annular photoreactor, a mass transport limited region ($Re < 100$) and a surface reaction limited region ($Re > 200$) were determined.

Toluene Studies

Ibusuki and Takeuchi investigated the photooxidation of trace 80 ppm toluene in air over UV irradiated TiO_2 at ambient temperature (20). The main product of the reaction at 10 min residence time was CO_2, with a trace (<2 ppm) of benzaldehyde as the only detected gas-phase intermediate. Water appears to be required for reaction: No reaction products or decrease of toluene concentration were detected in a toluene (80 ppm)–dry air system, and only a slight reactant decrease was noted in a toluene (80 ppm)–NO_2 (80 ppm)–dry air mixture. These authors observed that the batch photoreactor CO_2 concentration at 10 min residence time increased linearly with increasing relative humidity over the range 0–60%; thus, water vapor enhanced the photooxidation rate.

Suzuki *et al.* studied toluene photocatalytic deodorization of air on TiO_2-coated honeycomb ceramic monolith in a recirculation reactor system (21). The odor compounds examined individually included acetaldehyde, isobutyric acid, toluene, methyl mercaptan, hydrogen sulfide, and trimethylamine. They reported that these odor compounds disappeared via pseudo-first-order photooxidation kinetics. The photocatalytic monolith has been examined as an on-board car air purifier in new and used vehicles; its effectiveness has been evaluated through both chemical analysis and human panel tests (22) and a reactor model developed to include concentration, momentum, and illumination fields (23).

Most gas–solid photocatalytic oxidations discussed in the literature were exclusively limited to the single-component

TABLE 1

Photocatalytic Sensitization by TCE (24)

Compounds	Time for 90% conversion
Isooctane (0.115%)	22.5
Isooctane + 400 ppm TCE	7
Methylene chloride (0.75%)	550
Methylene chloride + 669 ppm TCE	300
Methylene chloride + 0.373% TCE	270
Methylene chloride + 0.752% TCE	155
Chloroform (2.3%)	720
Chloroform + 0.206% TCE	380

pollutant system; these provide convenient cases for understanding the kinetics of photocatalytic oxidation. For commercial photocatalysis application, a contaminated air stream will often contain more than one contaminant. Therefore, multicomponent system studies can help us understand photocatalytic oxidation under more realistic process conditions and ultimately provide a stronger photoreactor design basis.

Berman and Dong studied the individual photocatalytic oxidation for trichloroethylene, perchloroethylene, vinyl chloride, 1,2-dichloroethane, methyl chloroform, hexanes, methylene chloride, carbon tetrachloride, isooctane, methanol, ethanol, acetone, trioxane, benzene, and toluene in air in a continuous-flow reactor (24). They first reported that the individual isooctane, methylene chloride, and chloroform photocatalytic decomposition rates could be increased substantially with the addition of trichloroethylene to the system. Table 1 summarizes their published experimental results for an air stream containing 3% water and 0.115% isooctane or 0.75% methylene chloride or 2.3% chloroform at 30°C. They interpreted this rate promotion as caused by trichloroethylene providing Cl· atoms to initiate some (unstated) oxidative chain reactions of other compounds, but gave no mechanism, kinetic rate equation, or other multicomponent data to rationalize such an increase. While these authors termed the effect a "photosensitization," we prefer and use here a "chlorine promotion" effect, based on the presumed involvement of chlorine redicals.

We present below our initial study of both individual and simultaneous photocatalyzed conversion of TCE and toluene. Our individual reactant results show conventional Langmuir–Hinshelwood rates for toluene and the expected high rates (100% conversion) for TCE in a 5-ms residence time downflow powder bed reactor. The simultaneous conversion displays considerable surprise, including a chlorine promotion of toluene, which can reach 90–100% toluene conversion at low toluene concentrations, and conversely an efficient toluene "quench" of TCE conversion as the toluene level is raised above 120 mg/m^3. Finally, we explore alternate rationalizations for this novel behavior in terms of (i) a TCE chain mechanism, (ii) a new solid phase, and (iii) water influences.

2. EXPERIMENTAL

The photocatalyzed degradation of trace level trichloroethylene and toluene mixtures in air was carried out using near-UV-illuminated titanium dioxide (anatase) powder in a flow reactor, designed previously by Peral and Ollis to study photocatalytic oxidation kinetics of acetone, 1-butanol, butyraldehyde, formaldehyde, and *m*-xylene (25).

The catalyst used was P25 TiO_2 (Degussa), characterized by the manufacturer as having a primary particle diameter of 30 nm, a surface area of 50 m^2/g, and a crystal structure of primarily anatase. The catalyst particles were spherical and nonporous, with stated purity of >99.5% TiO_2. Stated impurities included: Al_2O_3 (<3%), HCl (<0.3%), SiO_2 (<0.2%), and Fe_2O_3 (<0.01%). This catalyst was used as supplied, without pretreatment. The trichloroethylene and toluene used to prepare individual gas mixtures were of HPLC grade, supplied by Aldrich and Fisher Scientific, respectively.

Gas concentrations were analyzed by gas chromatography (Perkin–Elmer Sigma 1) operating with a flame ionization detector (FID). An Alltech C-5000 column with AT-1000 Chromosorb W-AW 80/100 packaging was used for trichloroethylene and toluene analysis.

A 100-W black light (UVP) lamp was used to provide vertical near-UV illumination. The incident light intensity for the lamp was determined via ferrioxalate liquid actinometry to be 5.0×10^{-7} E/cm^2 min. All experiments were performed at 22–24°C.

In a typical experiment, 0.1 g TiO_2 powder was spread uniformly over the surface of the porous fritted glass plate, providing a 3.2-mm-deep TiO_2 powder layer. The 20.11-liter gas reservoir was filled to 1.013×10^{-4} N/m^2 with UHP air. A suitable amount of water and contaminant, each in liquid form, were each injected into the reservoir through a sample port. Following complete vaporization, the reservoir was filled with additional UHP air up to a final pressure (typically 2.18×10^5 N/m^2). Two streams flowing directly from the UHP air tank and the air–water vapor contaminant reservoir were mixed continuously and passed into the photoreactor. A mass flow controller (Linde FM4574) was used to provide the desired mass flow rates for both air and contaminant streams. The resultant contaminant and humidified air mixture was passed through the reactor for a considerable time until the feed and reactor exit gas concentrations were identical. Then the light was turned on, and gas samples were taken every 15 to 30 min. The exit gas concentration was carefully monitored until it reached the near-steady-state value. This photo-steady state was usually reached in 3–7 h for different contaminant concentrations. Between the kinetic runs, the TiO_2 catalyst was regenerated

through UV illumination with dry air passing through the reactor.

3. RESULTS

TCE and Toluene Individual Photooxidation

The purpose of this research is to study trichloroethylene and toluene mixture photooxidation in a powder bed flow reactor. It is essential that we first look into toluene and trichloroethylene single-component photooxidation kinetics separately.

As the literature reported, trichloroethylene photodegradation rate is very rapid, supposedly due to a Cl·-initiated chain reaction nature, which results in an unusually high quantum yield. In the powder bed flow reactor, we confirmed these high rate reports, finding that ~100% TCE conversion was achieved for all gas-phase concentrations examined, up to 753 mg/m^3 in air at 20% relative humidity.

At the same relative humidity, with gas-phase toluene concentrations of 80–550 mg/m^3, pseudo-steady conversions of 20 to 8%, respectively, were observed in the powder bed flow reactor.

To analyze the toluene photooxidation data, we consider the plug-flow integral analysis of Peral and Ollis for the downflow powder bed reactor (25). If we assume that toluene photooxidation also follows the Langmuir–Hinshelwood rate form, the gas-phase toluene concentration can be described as:

$$V\frac{dC}{dZ} = -\frac{kKC}{1+KC}, \qquad [1]$$

where V is the linear gas velocity, C is the gas-phase toluene concentration, k is the apparent reaction rate constant, K is the adsorption constant, Z is the vertical position in the TiO_2 catalyst layer (measured from the top). The apparent reaction rate constant k is a function of light intensity and thus catalyst bed depth. Equation [2] can be used to evaluate the reaction rate constant variation with Z:

$$k(Z) = k_0 e^{-\alpha\varepsilon Z}, \qquad [2]$$

where k_0 is the rate constant at surface ($I_0 = 5\times10^{-7}$ E/cm^2 min), α is a constant ($\alpha = 0.5$–1.0), ε is the extinction coefficient of TiO_2, taken as (10211 cm^{-1}). Inserting Eq. [2] into Eq. [1], we have

$$V\frac{dC}{dZ} = -\frac{k_0 e^{-\alpha\varepsilon Z}KC}{1+KC}. \qquad [3]$$

Integrating Eq. [3] and assuming complete light absorption in the TiO_2 layer gives

$$\frac{\ln C_0/C}{C_0 - C} = \frac{k_0 K}{\alpha\varepsilon V}\frac{1}{C_0 - C} - K. \qquad [4]$$

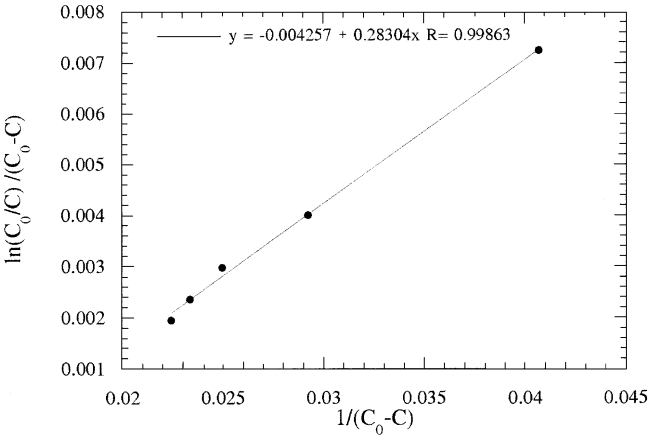

FIG. 1. Toluene photooxidation ($C_w = 1619.4$ mg/m^3).

If our rate form assumption is valid, the ln $C_0/C/(C_0-C)$ vs $1/(C_0-C)$ plot should be linear with a negative intercept, since the apparent adsorption constant K is always positive.

Figure 1 indicates a linear plot of the data; thus the Langmuir–Hinshelwood kinetic form combined with integral rate law analysis can be used to describe the toluene photooxidation rate (as found earlier for *m*-xylene). The k and K values calculated from the slope and intercept of the ln $C_0/C/(C_0-C)$ vs $1/(C_0-C)$ plot are

$$k = 3.14\ \text{g/liter min}$$
$$K = 0.00463\ \text{m}^3/\text{mg}.$$

Table 2 compares these toluene results with the values for *m*-xylene, acetone, and 1-butanol (25) photooxidation in the powder bed flow reactor. The toluene, *m*-xylene, and acetone have similar order magnitude of photodegradation rate constant and apparent binding constant, while the alcohol is most reactive.

For toluene concentration below 160 mg/m^3, the oxidation rate is approximately first order, whereas in the range of 160–550 mg/m^3, the oxidation rate is between zero and first order. The rate equation is

$$\text{rate} = \frac{3162\text{C}_{\text{tol}}}{1 + 0.00463\text{C}_{\text{tol}}}, \qquad [5]$$

TABLE 2

Photooxidation Rate Comparison in Powder Bed Reactor

Contaminants	Concentration (mg/m^3)	k (g/liter min)	K (m^3/mg)	Investigator
Toluene	80–550	3.14	0.0046	This study
m-Xylene	1–260	1.30	0.0066	(2, 25)
Acetone	1–260	7.75	0.0064	(2, 25)
1-Butanol	1–260	49.2	0.0011	(2, 25)

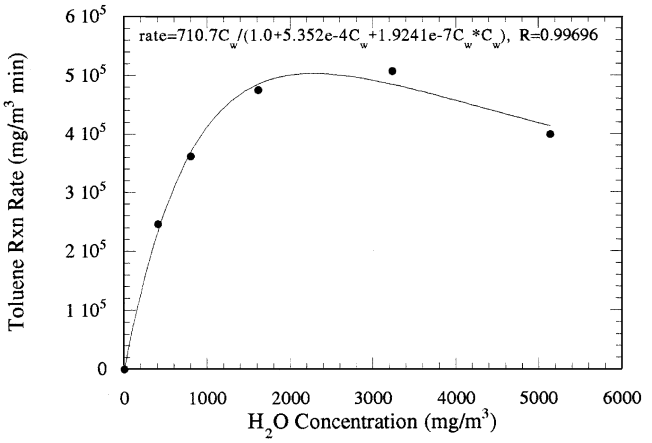

FIG. 2. Toluene reaction rate vs water concentration.

where the concentration unit is milligrams per cubic meter and the rate unit is milligrams per cubic meter per minute.

No intermediates were detected by gas chromatography with a flame ionization detector. Therefore, we believe that toluene degraded to form primarily carbon dioxide and water. This view is consistent with the findings of Ibusuki and Takeuchi, who reported that only a trace benzaldehyde (less than 1 ppm) appeared in the gas phase during photocatalytic conversion of 80 ppm toluene in humidified air; carbon dioxide was always the dominant product (20).

Water Influence on Toluene Photooxidation

The influence of water in photooxidation depends upon the contaminant. Water vapor strongly inhibits isopropanol (4, 5, 20), trichloroethylene (4, 5, 13–15, 20), and acetone oxidation (2); enhances toluene oxidation (1); has no significant effect on 1-butanol oxidation (2); and increases *m*-xylene oxidation rate up to 1500 mg/m^3 and decreases thereafter (2).

Figure 2 shows the measured toluene oxidation rate vs water concentration in the feed air stream. No toluene photodegradation proceeded in the total absence of water in the toluene–air mixture, as also observed by Ibusuki and Takeuchi (20). Toluene oxidation rate was enhanced by water concentrations up to 2000–3000 mg/m^3, which corresponded to about 23–40% relative humidity and was somewhat inhibited at 60% rh (6100 mg/m^3). For water concentration between 0 and 6000 mg/m^3, the water influence for toluene oxidation rate can be correlated as

$$\text{rate} = \frac{710.7 C_{\text{H}_2\text{O}}}{1 + 5.325 \times 10^{-4} C_{\text{H}_2\text{O}} + 1.9241 \times 10^{-7} C_{\text{H}_2\text{O}}^2}. \quad [6]$$

As with the previous equation [5], the concentration unit is milligrams per cubic meter and the rate unit is milligrams per cubic meter per minute.

Toluene Photooxidation in the Presence of Trichloroethylene

We showed above that toluene photooxidation follows the Langmuir–Hinshelwood form. Trichloroethylene photooxidation kinetic data have also to be fitted by such rate forms, with further modification to include strong water inhibition (13–20). Conventional competitive adsorption analysis for toluene and trichloroethylene in a two-contaminant mixture in air would predict that the photooxidation rate for both compounds should decrease.

We performed three sets of experiments at fixed water concentration in the feed stream.

(1) Fixed trichloroethylene concentration at 753 mg/m^3, varied toluene concentration from 80 to 550 mg/m^3;
(2) fixed trichloroethylene concentration at 226 mg/m^3, varied toluene concentration from 80 to 550 mg/m^3;
(3) fixed toluene concentration at 134 mg/m^3, varied trichloroethylene concentration from 220 to 760 mg/m^3.

Experimental results for these mixed reactant feeds are plotted in Figs. 3–8. No intermediates were detected by GC–FID for our toluene and trichloroethylene mixtures after photocatalyzed oxidation. In all three experiment sets, we observed a region where the toluene conversion increased markedly with the addition of trichloroethylene and another where the trichloroethylene conversion decreased strongly with increasing toluene levels, compared to the conversions achieved for single component toluene or trichloroethylene photooxidations, respectively. When the trichloroethylene/toluene ratio was increased, the toluene conversion increased dramatically at a certain threshold, and at the same time, trichloroethylene conversion also increased. The photooxidation rates behaved similarly.

Toluene and trichloroethylene oxidation conversion (Fig. 3) decreases with increasing toluene concentration at a fixed trichloroethylene level of 753 mg/m^3. When the toluene concentration is below 100 mg/m^3, both toluene

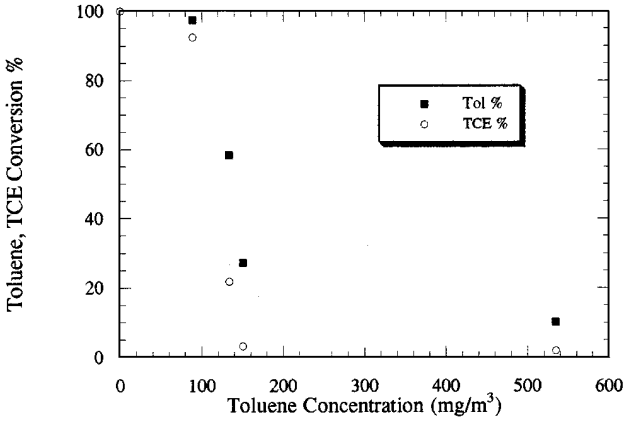

FIG. 3. Toluene, TCE conversions ($C_{\text{tce}} = 753.09$ mg/m^3).

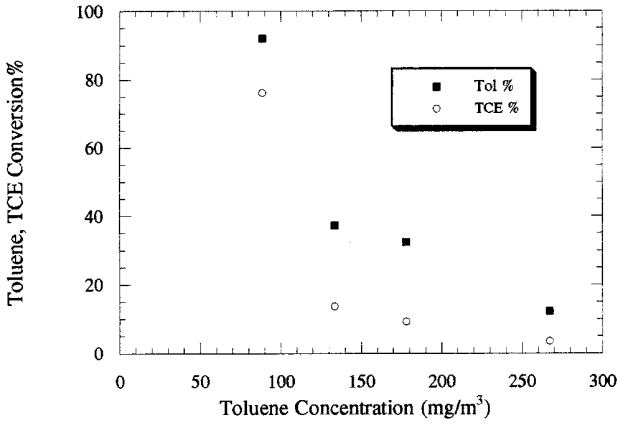

FIG. 4. Toluene, TCE conversions ($C_{tce} = 225.93$ mg/m^3).

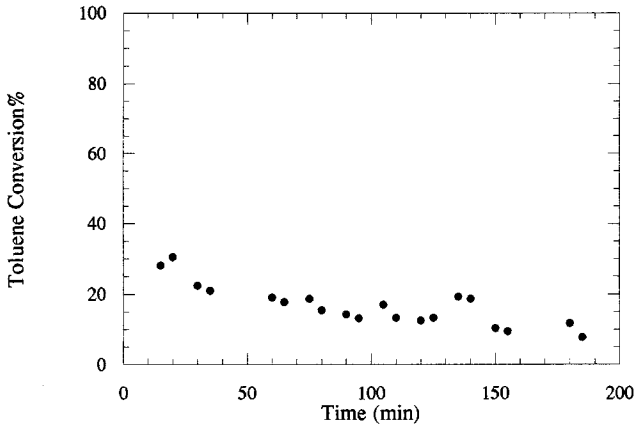

FIG. 6. Toluene conversion vs time ($C_{tol} = 534.57$ mg/m^3).

and trichloroethylene underwent almost complete photodegradation. At toluene concentrations above 160 mg/m^3, trichloroethylene was hardly converted, and only a slight toluene conversion increase in the mixture was observed, compared to the toluene single-component photooxidation.

A survey of air stripper effluents for remediation of trichloroethylene-contaminated ground water found trichloroethylene concentrations to be frequently around 100–200 mg/m^3 (26), although some sample sites might have trichloroethylene concentrations up to 6000 mg/m^3. Figure 4 shows toluene and trichloroethylene oxidation conversions at fixed trichloroethylene concentration of 226 mg/m^3. Toluene and trichloroethylene conversions drop dramatically when the toluene concentration is higher than 88 mg/m^3, corresponding to a trichloroethylene/toluene mass ratio near 3.

For trichloroethylene concentration varying from 220 to 760 mg/m^3 and toluene concentration below 88 mg/m^3, both trichloroethylene and toluene were completely converted; when the toluene concentration was above 160 mg/m^3, the toluene conversion dropped sharply to near its single-component value, and the trichloroethylene conversion was remarkably low, typically less than 5%.

Figure 5 compares toluene oxidation conversions and rates for three cases: toluene single component, toluene with 225.93 mg/m^3, and 753 mg/m^3 trichloroethylene, respectively. Trichloroethylene presence enhances toluene conversion, for all toluene concentrations below about 200 mg/m^3, and essentially total toluene conversion is found at toluene levels below 90 mg/m^3. Above 200 mg toluene/m^3, the presence of 89–753 mg/m^3 trichloroethylene was without influence on toluene conversions.

TiO_2 Catalyst Activity

Time-dependent TiO_2 catalyst activity was observed during powder bed flow reactor experiments. In the trichloroethylene single-component system, TiO_2 short-term activity increased with photooxidation reaction time (Fig. 6).

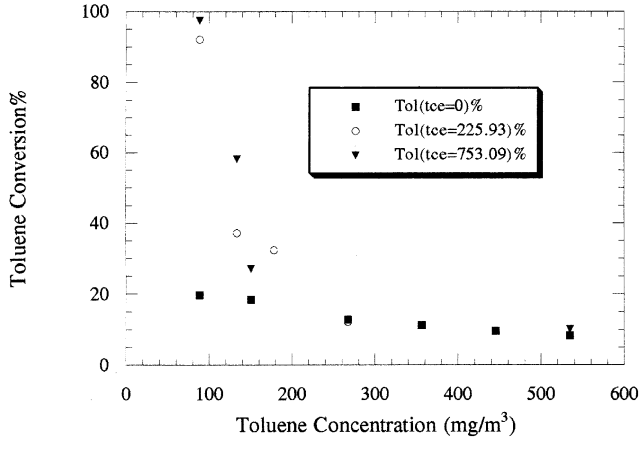

FIG. 5. Toluene conversions with or without TCE.

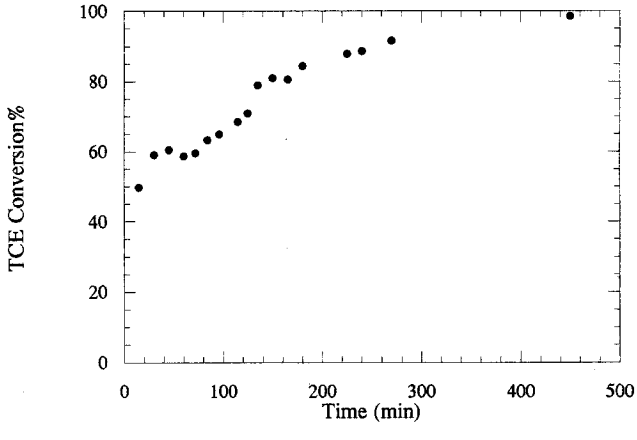

FIG. 7. TCE conversion vs time ($C_{tce} = 753.09$ mg/m^3).

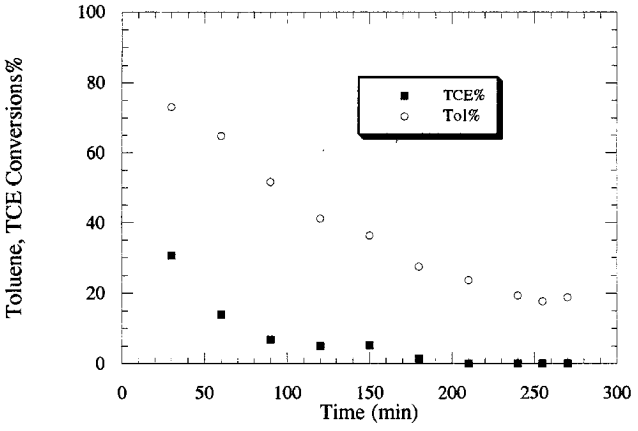

FIG. 8. Toluene, TCE conversions vs time ($C_{tce} = 753.09$ mg/m^3), $C_{tol} = 150.57$ mg/m^3).

Catalyst deactivation was observed during toluene photooxidation. For toluene photooxidation with or without trichloroethylene presence, TiO_2 activity decreased with time (Fig. 7 (no TCE), Fig. 8 (113.6 mg/m^3 TCE)). In the presence of trichloroethylene, the TiO_2 catalyst could be regenerated via UV illumination with flowing dry air through the reactor for longer than 3 h. An experiment was designed to compare catalyst activity decline of fresh and regenerated catalyst in the presence of TCE. Figure 9 shows toluene conversion for fresh catalyst (solid circle, increasing conversion with time, approaching 100% after 150 min); catalyst regenerated after 35 h continuous illumination (open circle, conversion = 85–93% after 270 min); and catalyst regenerated after seven successive use/regeneration cycles (solid diamond). At each intervening time the catalyst was illuminated for approximately 5 h. The fresh catalyst and catalyst regenerated after long-term (35 h) continuous illumination gave similar toluene conversions. After seven successive use and regeneration cycles (diamond), however, the TiO_2 catalyst deactivated considerably and could no longer be regenerated simply under UV illumination and dry air flow. This result probably indicates the eventual accumulation of some adsorbed species, which is not easily oxidizable.

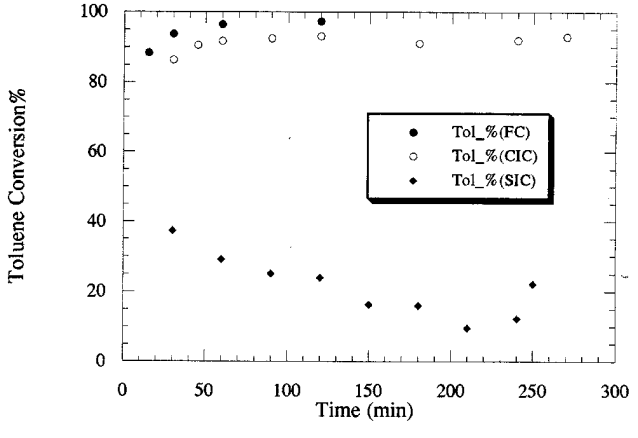

FIG. 9. Catalyst activity test for toluene conversion ($C_{tce} = 753.09$ mg/m^3, $C_{tol} = 88.48$ mg/m^3).

4. DISCUSSIONS

TCE and Toluene Reaction Pathways

It is well accepted that when TiO_2 particle is illuminated by wavelength <370 nm, the valence band electrons of the TiO_2 can be excited to the conduction band, creating highly reactive electron (e^-) and hole (h^+) pairs. Those electrons and holes migrate to the TiO_2 solid surface and are trapped at different sites. The first electron transfer products for gas–solid photocatalysis are the oxygen species O_2^- or O^- on the surface. The photogenerated holes may be trapped by hydroxyl ions or water on the surface to form hydroxyl radicals (1–5, 2, 13–15, 19, 20, 25–31). The initial reaction steps for the above mechanisms may be summarized as the following:

$$TiO_2 + h\nu \leftrightarrow h^+ + e^-$$
$$h^+ + OH^- \rightarrow OH\cdot$$
$$Ti^{4+} + e^- \rightarrow Ti^{3+}$$
$$Ti^{3+} + O_2 \rightarrow Ti^{4+} + O_2^-.$$

A number of homogeneous photochemical oxidations of toluene have been carried out in the presence of NO, NO_2, and air to simulate smog formation conditions. The homogeneous reaction is believed to be initiated by OH radical generated via the photodecomposition of nitrous acid. Two reaction mechanisms have been proposed, based respectively on the addition of OH radical to aromatic rings and the OH radical abstraction of hydrogen from the alkyl group (6, 32–34). The yield for each homogeneous pathway was reported by several authors (35–38). The abstraction pathway yield ranged from 0.08 to 0.16, and that for addition varied from 0.92 to 0.84.

Ibusuki and Takeuchi (20) studied trace (80 ppm) toluene-photocatalyzed oxidation in air with and without 80 ppm NO_2 presence. Without NO_2 presence, only CO_2 and trace benzaldehyde (<1 ppm concentration) were noted as the products. They reported that the CO_2 formation rate increased linearly with rising relative humidity and that trace benzaldehyde yield decreased with increasing relative humidity. They concluded that the increasing gas-phase H_2O concentration probably increased the surface OH^- concentration and thus surface ·OH levels.

The trichloroethylene homogeneous photooxidation reaction has been studied extensively. Although the exact reaction mechanism is still under investigation, it seems agreed that trichloroethylene undergoes a chain reaction that results in a quantum efficiency greater than 1. Sanhueza

et al. (39, 40) proposed a chain reaction mechanism that involved Cl· atoms attacking trichloroethylene to initiate the oxidation reaction. The Cl· atoms required for the TCE photooxidation reaction were produced by an initiation reaction involving trichloroethylene (41).

The existence of quantum yields greater than 1.0 for the photocatalyzed destruction of TCE leads to the supposition that the photocatalyzed reaction must be (primarily) a chain reaction also. The observation of dichloroacetylchloride ($CHCl_2CCl_2(O)$) as a major intermediate suggests that a Sanhueza-like chain mechanism may occur on illuminated photocatalyst.

The Sanhueza *et al*. mechanism:

$$\begin{aligned} CCl_2CHCl + Cl\cdot &\rightarrow CHCl_2CClCl\cdot \\ CHCl_2CClCl\cdot + O_2 &\rightarrow CHCl_2CCl_2OO\cdot \\ 2CHCl_2CCl_2OO\cdot &\rightarrow 2CHCl_2CCl_2O\cdot + O_2 \\ CHCl_2CCl_2O\cdot &\rightarrow CHCl_2CCl(O) + Cl\cdot \end{aligned}$$

or a minor pathway may take place

$$CHCl_2CCl_2O\cdot \rightarrow CHCl_2\cdot + CCl_2.$$

The Cl· radicals required on the TiO_2 surface may arise from the hydroxyl radicals or oxygen atoms produced by TiO_2. The production of oxygen atoms on TiO_2 has often been invoked in the gas–solid heterogeneous photocatalytic oxidation of organics (42), and oxygen atoms formed on the TiO_2 surface could react with trichloroethylene.

Similarly the hydroxyl radical is known to be produced on TiO_2 wet surface under UV illumination (31), and hydroxyl radical reactions with trichloroethylene could release chlorine radicals, à la the gas-phase reactions of Kleingienst *et al*. (41). In either case, for the photocatalyzed trichloroethylene conversion, the likely source for the Cl· atoms is the reaction of trichlorethylene with photocatalytically produced radicals to produce the observed intermediate, dichloroacetaldehyde chloride (19):

$$\begin{aligned} CCl_2CHCl + \cdot OH &\rightarrow \cdot CCl_2CHClOH \\ \cdot CCl_2CHClOH + O_2 &\rightarrow \cdot OOCCl_2CHClOH \\ 2\cdot OOCCl_2CHClOH &\rightarrow 2\cdot OCCl_2CHClOH + O_2 \\ \cdot OCCl_2CHClOH &\rightarrow CHClOHCCl(O) + Cl\cdot. \end{aligned}$$

A possible route for the reaction of the intermediate DCAC to produce a second observed intermediate, phosgene, Cl_2CO, is given by Jacoby (19):

$$\begin{aligned} OH\cdot + CHCl_2CCl(O) &\rightarrow \cdot CCl_2Cl(O) + H_2O \\ O_2 + \cdot CCl_2CCl(O) &\rightarrow \cdot OOCCl_2CCl(O) \\ 2\cdot OOCCl_2CCl(O) &\rightarrow 2\cdot OCCl_2CCl(O) + O_2 \\ \cdot OCCl_2CCl(O) &\rightarrow CCl_2O + CClO\cdot \\ CClO\cdot &\rightarrow Cl\cdot + CO. \end{aligned}$$

Jacoby carried out a detailed study of the photocatalyzed destruction of trichloroethylene in air in a TiO_2 surface (19). He proposed two reaction pathways for TCE photooxidation. In pathway A, the reaction proceeds through the DCAC intermediate, and in pathway B, trichloroethylene is oxidized directly to products. Experimentally, Jacoby observed that up to 85% of reacted trichloroethylene was converted through the DCAC pathway. He further concluded by addition of ethane as a "quenching" agent that trichloroethylene oxidation was taking place exclusively on the TiO_2 surface, i.e., no gas-phase chain reaction was occuring.

The chain reaction notion thus appears for two basic reasons:

(i) high observed quantum yields, exceeding unity and
(ii) high intermediate levels of DCAC, known to be produced in gas-phase photochemistry via a Cl·-driven chain reaction.

We discuss below a potential chain reaction for toluene/TCE mixtures, which could rationalize our observed promotion and inhibition effects.

Catalyst Deactivation

Photocatalyst deactivation during alcohol oxidation was first reported by Cunningham and Hodnett (7), who examined 2-butanol, 2-propanol, and 1-butanol over illuminated TiO_2 and ZnO at alcohol concentration ranges 160–20000 mg/m^3. Catalyst deactivation profiles were similar for different alcohol concentrations. The authors suggested that the CO_2 product formed during reaction absorbed on the catalyst surface and competed for the catalyst active sites.

However, since all photocatalyzed oxidations of carbonaceous reactants produce CO_2, but only certain reaction systems exhibit catalyst deactivation phenomena, it appears more likely that some less general inhibitory products or recalcitrant intermediates are formed during reaction and remain absorbed on the catalyst surface. These intermediates are presumably responsible for catalyst deactivation. For example, Blake and Griffin proposed a 1-butanol photooxidation mechanism in which they speculated that butanoic acid was gradually formed from adsorbed butyraldehyde during photooxidation reaction, in order to rationalize the slow appearance of carboxylate IR bands (10). They further stated that the presumed butanoic acid was strongly absorbed on the TiO_2 surface and that such acid accumulation was responsible for the slow catalyst deactivation observed. The catalyst deactivation could be enhanced during each dark period, presumably by the dark, facile oxidation of the remaining adsorbed butyraldehyde to butanoic acid. They suggested that on the TiO_2 surface, a hole attack on the adsorbed carboxylate caused photocatalyzed decarboxylation, thereby regenerating the catalyst activity in the

absence of further reactant alcohol:

$$RCOO^- + h^+ \rightarrow RCOO\cdot \rightarrow CO_2 + R\cdot$$
$$\rightarrow \text{gaseous products.}$$

In our experiments with simultaneous toluene and trichloroethylene photocatalyzed oxidation, no intermediates were found by GC with a FID detector. Toluene photooxidation takes place on the TiO_2 surface and follows the Langumir–Hinshewood kinetics form. A used TiO_2 catalyst was suspended in methanol to extract any adsorbed oxygenates, and the resultant solution was examine by UV spectrum. This spectrum verified that some methanol-extractable intermediates are formed during toluene photooxidation and remain absorbed on the TiO_2 surface. Further mass spectrum analysis (NCSU) indicated the major absorbed intermediate to be benzoic acid. We suggest that this absorbed benzoic acid is the oxidation product of benzaldehyde, which would be consistent with both Ibusuki's observation of trace benzaldehyde gas-phase appearance during toluene oxidation and Blake and Griffin's claim that adsorbed butyraldehyde can be converted to the corresponding carboxylic acid.

Like Blake and Griffin's claim that adsorbed carboxylic acid inhibited butanol conversion, we suggest that accumulated benzoic acid inhibits toluene and trichloroethylene photooxidation rates. This view also helps to explain the TiO_2 catalyst activity decreases during toluene and trichloroethylene photooxidation in high toluene (>200 mg/m^3) atmospheres.

Coulpling of TCE and Toluene Oxidations

To explain our toluene/TCE results, we need to postulate a coupling between the stoichimetric toluene conversion and the assumed chain reaction model for TCE destruction. This coupling must rationalize

(i) toluene rate enhancement by TCE at low toluene level and
(ii) toluene quenching of TCE conversion at high toluene levels.

A useful example for discussion is a network that includes a chain mechanism for TCE conversion and a chain transfer step for toluene involvement:

Toluene (nonchain sequence)

$$TiO_2 + OH^- + h\gamma \rightarrow \cdot OH$$
$$\cdot OH + \phi CH_3 \rightarrow \phi CH_2\cdot + H_2O$$
$$\phi CH_2 + (O_2, \cdot OH) \rightarrow CO_2$$

TCE (chain) initiation

$$TCE + TiO_2 + h\gamma \rightarrow Cl\cdot + \cdots$$

Propagation

$$TCE + Cl\cdot \rightarrow CHCl_2CCl_2\cdot$$
$$CHCl_2CCl_2\cdot + O_2 \rightarrow CHCl_2CCl_2OO\cdot$$
$$2CHCl_2CCl_2OO\cdot \rightarrow 2CHCl_2CCl_2O\cdot + O_2$$
$$CHCl_2CCl_2O\cdot \rightarrow CHCl_2CCl(O) + Cl\cdot$$

Termination (example)

$$Cl\cdot + H_2O \rightarrow \cdot OH + HCl \text{ (presence of } H_2O)$$
$$2Cl\cdot \rightarrow Cl_2 \text{ (absence of } H_2O)$$

Chain transfer

$$Cl\cdot + \phi CH_3 \rightarrow \phi CH_2\cdot + HCl$$

This example mechanism is consistent with the following experimental observations:

(1) For TCE/air feeds, 100% conversion has been achieved in 5–6 ms at all concentrations studied (up to 753 mg/m^3), which suggests a long reaction chain.

(2) With low toluene addition to the TCE/air system, Cl· activates $C_6H_5CH_3$ by chain transfer and thus increases the toluene rate and conversion dramatically; sufficient Cl· remains to maintain a TCE chain length sufficient to give 100% conversion.

(3) With higher toluene addition to the TCE/air system, toluene consumes sufficient Cl· to terminate the chain reaction, therefore sharply inhibiting TCE reaction.

The mechanism of further conversion of the aromatic intermediates is unknown on the TiO_2 surface, but suggestions may again be found from gas-phase chemistry. For example, Atkinson *et al.* postulated the following steps to explain the gas-phase α-dicarbonyl reaction (36).

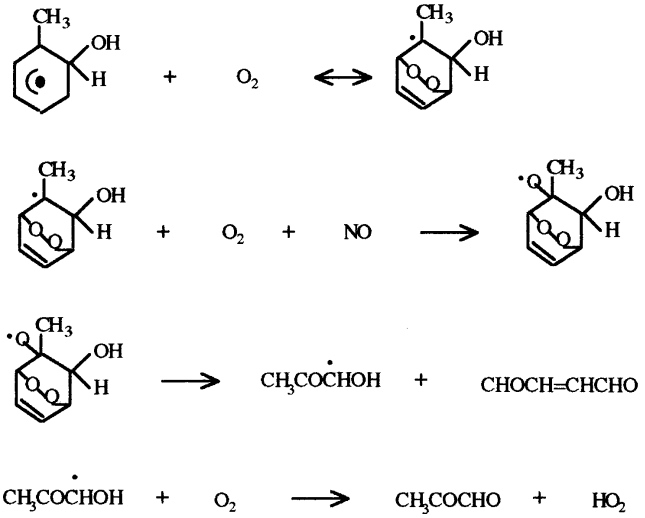

The α-dicarbonyl gas-phase yield is about 25–29% for toluene. From GC–MS and MS–MS analysis, a variety

of other ring cleavage products are identified, including: $CH_3COCOCH{=}CH_2$, $CHOCOCH{=}CH_2$, $CH_3COCH{=}CH_2$, $CH_3COCH{=}CHCH{=}CH_2$, $CHOC(OH){=}CHCHO$, and $CH_3COCH{=}CHCH{=}CHCHO$.

Similar ring cleavage processes may exist on the illuminated TiO_2 surface for toluene due to the existence of the radical OH· and initiator Cl· and the presence of molecular oxygen, O_2. The α-dicarbonyl or other unsaturated ring cleavage products formed can be further photooxidized rapidly to the final products, CO_2 and H_2O. This kinetic possibility may rationalize why no appreciable gas-phase intermediates and reaction products were detected by GC/FID. It is also consistent with earlier observations by Teichner and Formenti (42) that photocatalyzed oxidation of small olefins produces primarily carbon dioxide.

Other mechanistic possibilities are noted:

(i) The TiO_2 surface may become sufficiently chlorinated to yield a new surface, or even bulk phase; Primet *et al.* (1) have shown that carbon tetrachloride reacts easily with surface oxygen atoms at very modest temperatures (150°C), and such new phases may have desirable catalytic properties, e.g., forming Cl radicals, and reducing or eliminating undesired electron/hole recombinations.

(ii) The influence of water remains unclear. Complete oxidation of TCE consumes water, while toluene conversion to CO_2 produces water. Dibble and Raupp (14) found that excess water inhibits TCE conversion strongly. Thus, the high rate to low rate transition seen on increasing toluene could be a switch from a "trace water" system to an "excess water" system. Further studies are clearly needed to sort out these and yet other possibilities.

5. CONCLUSIONS

Trichloroethylene and toluene in humidified air could be individually photocatalytically oxidized by near-UV illumination and TiO_2 catalyst in a powder bed flow reactor with residence time only about 5.6 ms. Trichloroethylene photooxidation was very rapid under our experimental conditions, and ~100% conversion was achieved for all trichloroethylene concentrations examined up to 753 mg/m^3. The toluene photodegradation rate was successfully fitted by Langmuir–Hinshelwood form. Toluene oxidation rates were of the same order magnitude as *m*-xylene and acetone. No toluene photooxidation intermediates were detected; we believe that toluene was eventually converted to carbon dioxide. Water vapor presence was essential for toluene oxidation, as no toluene degradation was observed in the complete absence of water vapor in the feed stream. Toluene oxidation rate increased with water concentration up to 1650 mg/m^3 (20% relative humidity) and decreased thereafter.

The photooxidation kinetics of trichloroethylene and toluene mixtures in humidified air exhibited strong promotion and inhibition behavior vs that expected from individual single-reactant kinetic degradation data. The presence of sufficient trichloroethylene enhanced the toluene photooxidation rate and allowed achievement of 90–100% toluene conversion, when toluene feed levels were below about 120 mg/m^3. These results constitute the first report of (near) total conversion at short residence times of an aromatic hydrocarbon, which presently represents a very important air emission problem. A global mechanism is suggested that incorporates the individual nonchain and chain mechanisms thought to occur with toluene and TCE individual conversions, respectively.

Time-dependent catalyst activation and deactivation were observed. At first, a deactivated catalyst could be regenerated under UV illumination and dry air flow. Eventually, catalyst deactivation becomes irreversible. While carboxylate formation and carboxylic acid accumulation could be a major cause of deactivation, the full picture here has yet to be elucidated.

ACKNOWLEDGMENTS

This work was supported by NASA Research Grant NAG 2-684. We are pleased to acknowledge NASA's strong interest in multicomponent conversions as a primary motivator for our exploration of the TCE enhanced oxidation of toluene.

REFERENCES

1. Primet, M., Basset, J., Mothien, M. V., and Prettre, M., *J. Phys. Chem.* **79**, 2868 (1970).
2. Djeghri, N., Formenti, M., Juillet, F., and Teichner, S. J., *Faraday Discuss. Chem. Soc.* **58**, 185 (1974).
3. Djeghri, N., and Teichner, S. J., *J. Catal.* **62**, 99 (1980).
4. Bickley, R. I., and Stone, F. S., *J. Catal.* **31**, 389 (1973).
5. Bickley, R. I., Munuera, G., and Stone, F. S., *J. Catal.* **31**, 398 (1973).
6. Gratzel, M., Thampi, K. R., and Kiwi, J., *J. Phys. Chem.* **93**, 4128 (1989).
7. Cunningham, J., and Hodnett, B. K., *J. Chem. Soc. Faraday Trans. 1* **77**, 2777 (1980).
8. Mozzanega, H., Herrmann, J., and Pichat, P., *J. Phys. Chem.* **183**, 2251 (1979).
9. Sato, S., *J. Phys. Chem.* **87**, 3531 (1983).
10. Childs, L. P., and Ollis, D. F., *J. Catal.* **67**, 35 (1981).
11a. Blake, N. R., and Griffin, G. L., *J. Phys. Chem.* **92**, 5697 (1988).
11b. Peral, J., and Ollis, D. F., "The First International Conference on TiO_2 Photocatalytic Purification and Treatment of Water and Air, London, Ontario, Canada," p. 741. Elsevier, Amsterdam/New York 1993.
12. Ponder, W. H., "EPA's Pollution Prevention Research Program in the Air and Energy Engineering Laboratory's Organics Control Branch," Presentation, Air and Energy Engineering Research Laboratory. United States Environmental Protection Agency, Washington, DC, 1994.
13. Dibble, L. A., Ph.D. Dissertation, Arizona State University, 1989.
14. Dibble, L. A., and Raupp, G. B., *Catal. Lett.* **4**, 345 (1990).
15. Dibble, L. A., and Raupp, G. B., *Environ. Sci. Technol.* **26**, 492 (1992).
16. Nimlos, M. R., Jacoby, W. A., Blake, D. M., and Milne, T. A., "The First International Conference on TiO_2 Photocatalytic Purification and Treatment of Water and Air, London, Ontario, Canada," p. 387. Elsevier, Amsterdam/New York, 1993.

17. Holden, W., Marcellino, A., Valic, D., and Weedon, A. C., "The First International Conference on TiO_2 Photocatalytic Purification and Treatment of Water and Air, London, Ontario, Canada," pp. 393. Elsevier, Amsterdam/New York, 1993.
18. Anderson, M. A., Yamazaki-Nishida, S., and Cervera-March, S., "The First International Conference on TiO_2 Photocatalytic Purification and Treatment of Water and Air, London, Ontario, Canada," p. 405. Elsevier, Amsterdam/New York, 1993.
19. Jacoby, W. A., Ph.D. Dissertation, University of Colorado, 1993.
20. Ibusuki, T., and Takeuchi, K., *Atmos. Environ.* **20**, 1711 (1986).
21. Suzuki, K., Satoh, S., and Yoshida, T., *Denki Kagaku* **59**, 512 (1991).
22. Suzuki, K., "The First International Conference on TiO_2 Photocatalytic Purificaton and Treatment of Water and Air, London, Ontario, Canada," p. 421. Elsevier, Amsterdam/New York, 1993.
23. Luo, Y., Ph.D. Dissertation, North Carolina State University, 1994.
24. Berman, E., and Dong, J., "The Third International Symposium Chemical Oxidation: Technology for the Nineties, Vanderbilt University, Nashville, Tennessee," Vol. 3, p. 133. Technomic Publishing, 1993.
25. Peral, J., and Ollis, D. F., *J. Catal.* **136**, 554 (1992).
26. Miller, R., and Fox, R., "The First International Conference on TiO_2 Photocatalytic Purification and Treatment of Water and Air, London, Ontario, Canada," p. 573. Elsevier, Amsterdam/New York, 1993.
27. Munuera, G., Rives-Arnau, V., and Saucedo, A., *J. Chem. Soc. Faraday Trans. 1* **75**, 736 (1979).
28. Gonzalez-Elipe, A. R., Munuera, G., and Soria, J., *J. Chem. Soc. Faraday Trans. 1* **75**, 748 (1979).
29. Primet, M., Pichat, P., and Mathieu, J., *J. Phys. Chem.* **75**, 1216 (1971).
30. Primet, M., Pichat, P., and Mathieu, J., *J. Phys. Chem.* **75**, 1221 (1971).
31. Anpo, M., Shima, T., and Kubokawa, Y., *Chem. Lett.* 1799 (1985).
32. Hoshino, M., Akimoto, H., and Okuda, M., *Bull. Chem. Soc. Japan* **51**, 718 (1978).
33. Kenley, R. A., Davenport, J. E., and Hendry, D. G., *J. Phys. Chem.* **82**, 1095 (1978).
34. Atkinson, R., *Chem. Rev.* **85**, 69 (1985).
35. Gery, M. W., Fox, D. L., Stockburger, L., and Weathers, W. S., *Int. J. Chem. Kinet.* **17**, 931 (1985).
36. Atkinson, R., Carter, W. P. L., and Winer, A. M., *J. Phys. Chem.* **87**, 1605 (1983).
37. Kenley, R. A., Davenport, J. E., and Hendry, D. G., *J. Phys. Chem.* **85**, 2740 (1981).
38. Perry, R. A., Atkinson, R., and Pitts, J. N. J., *J. Phys. Chem.* **81**, 296 (1977).
39. Sanhueza, E., and Heicklen, J., *J. Phys. Chem.* **79**, 7 (1975).
40. Sanhueza, E., Hisatsune, J., and Heicklen, J., *Chem. Rev.* **76**, 801 (1976).
41. Kleingienst, T. E., Shepson, P. B., Nero, C. M., and Bufalini, J. J., *Int. J. Chem. Kinet.* **21**, 863 (1989).
42. Teichner, S. J., and Formenti, M., "Heterogeneous Photocatalysis, Photoelectrochemistry Photocatalysis and Photoreactors." Reidel, Dordrecht, 1985.